Experiment and fitting calculation of migration critical velocity of small-sized sediment particles erosion in rainwater pipeline

Cuiyun Liu, Yanzhi Chen, Yuting Yang, Jingqin Zhou, Yiyang Wang, Jie Zhou and Xiaohua Zhang

ABSTRACT

The migration critical velocity of small-sized sediment particles was investigated through experiments under different particle sizes, pipe wall roughness, and sediment thickness. Such experiments were carried out to simulate the erosion process of small-sized sediment particles in a rainwater pipeline during rainfall. The mathematical models were established via quadratic fitting to calculate the critical velocity of migration. Results showed that small particles had powerful cohesive force, and aggregates had strong erosion resistance. So, for the small-sized particles (in the range of 0.33–0.83 mm), the smaller the particle size, the larger the critical velocity. When the pipe wall roughness was large, the 'starting' particle resistance was high. A large flow dynamic was needed to overcome such resistance. Thus, the critical velocity was great. The critical velocity was also large when the sediment thickness was large. The difference rate between the critical velocity calculated by mathematical models and the measured value was within the range of −3.60% to 5.33% and had good consistency. Under the research conditions, the critical velocity ranges of the four commonly used pipes; namely, plexiglass, steel/PVC, galvanized/clay, and cast iron pipes, were calculated.

Key words | critical velocity, erosion process, migration, rainwater pipeline, sediment particles

Cuiyun Liu (corresponding author)
Yanzhi Chen
Yuting Yang
Jingqin Zhou
Yiyang Wang
Jie Zhou
Xiaohua Zhang
College of Urban Construction,
Nanjing Tech University,
Nanjing 211816,
China
E-mail: *yunduobai@126.com*

HIGHLIGHTS

- The aggregates of small particles in rainwater pipes have strong erosion resistance.
- The critical velocity is great when particle size is small (d50 = 0.33–0.83 mm).
- Critical velocity significantly decreases when the pipe wall roughness reduces.
- Difference rate between calculated and measured values is from −3.60% to 5.33%.
- The critical velocity ranges of the four commonly used pipes have been calculated.

doi: 10.2166/ws.2020.341

GRAPHICAL ABSTRACT

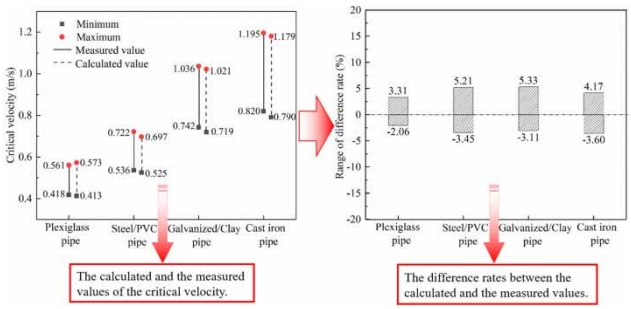

INTRODUCTION

Sediments in rainwater pipelines can be easily washed up and carried away during rainy days. Among the various substances of urban stormwater pollutants, the suspended solids, heavy metals, and polycyclic aromatic hydrocarbons (PAHs) are considered the major causes of contamination in receiving environments (Zoppou 2001; Fletcher *et al.* 2013).

Previous research on the erosion process of sediments in drainage pipes focused on the exploration of the dynamic migration of sediments in pipes under different conditions. Sediment transport regularity in pipelines was simulated over time with an artificial neural network (Ebtehaj & Bonakdari 2013). Nonlinear regression and MINITAB software were used to predict sediment migration under different conditions, involving few parameters and rapid calculation (Ebtehaj *et al.* 2014). Gene expression programming was used to simulate the movement of suspended particles or sediments in pipelines (Ab. Ghani & Md. Azamathulla 2011). Sediment particle and sphere velocity measurements were carried out in two pipe channels, and a semi-theoretical equation was established for sediment transport at the limit of deposition in sewers (Ota & Perrusquia 2013). The raw acoustical turbidity was used as an online monitoring tool, and the accurate suspended solids concentration and water height could be obtained through this approach (Pallarès *et al.* 2016). The erosion or deposition process in a sewer channel in Paris were monitored for a long period of time during rainfall. Results showed that sediments with small particle size (<4.15 mm) were likely to be washed out (Shahsavari *et al.* 2017).

The sediment in pipelines was continuously washed, and the change in the height of sediment was measured to determine the conditions of sediment erosion and transport (Campisano *et al.* 2004). The critical shear stresses of sediment at different erosion velocities in a sewer were determined (Hrissanthou & Hartmann 1998). The transport capacity of the sediment in the pressure drainage pipe was poor. The sediment showed signs of starting to migrate at a velocity of 0.35 m/s, and significant migration occurred at 0.50 m/s (Gunkel & Pawlowsky-Reusing 2017). In studying the 'starting' process of sediment particles in drainage pipelines, the movement of riverbed sediments and the erosion of ground particles by rain can be identified. A small amount of sediment movement was observed on the bed during the evaluation of the criteria for the riverbed sediment to start (He *et al.* 2002).

When the flow velocity exceeds a certain limit, the sediment particles will migrate. This limit is the 'starting velocity', which is called the 'critical velocity' of sediment particle migration. In theory, the particles cannot be washed out when the flow velocity is lower than the 'critical velocity'.

In this study, the erosion process of sediment particles in a rainwater pipeline was simulated in the laboratory during rainfall. The migration critical velocity of small-sized sediment particles was investigated under different particle sizes, pipe wall roughness, and sediment thickness. On this basis, mathematical models were established to calculate the critical velocity of sediment particles when being eroded in sewers under certain conditions. This approach helps control sediment pollution in urban drainage pipes.

MATERIALS AND METHODS

Reactor

Figure 1 presents the device used for simulating the erosion migration process of sediment particles in a rainwater pipeline. The plexiglass pipe has a length of 2 m and a diameter of 150 mm. The test pipe was connected to the bottom of a water tank, and the pipe flow was controlled through the valve and flow meter at the beginning of the pipe. The water flow velocity was measured by a velocity instrument. To facilitate the placement of sediment particles in the pipe, grooves were made at the top of the pipe. The sand paper, with a width of 12 cm, was laid on the inner wall of the pipe to simulate the commonly used drainage pipe materials. The grit size of sand paper was determined according to the roughness of different pipes. Table 1 illustrates the pipe, wall roughness, and the corresponding grit size of sand paper. Roughness is measured with a roughness tester.

The sediments used in the experiment were taken from outdoor rainwater drains. Such sediments were air-dried to constant weight, and the sediment particles with different sizes were sieved with a mesh sieve. At the beginning of the experiment, sediment of a certain mass and particle size was weighed and evenly mixed with a certain volume of water. The wet sediments were evenly smeared on the inner wall within the range of 1.00–1.25 m at the beginning of the pipeline, with a thickness between 0.20 cm and 0.35 cm. The valve was opened to a certain flow level, and sampling was conducted at 0, 15, 30, 45, and 60s at the outlet of the pipe. Then, the suspended solids (SS) concentration of the samples was measured. The experiments were completed considering changes in particle sizes, pipe wall roughnesses, and sediment thicknesses.

Table 1 | Pipe, roughness, and the corresponding grit size of the sand paper

Pipe	Roughness (μm)	Grit size of sand paper (mesh)
Cast iron pipe	250	60
Galvanized/clay pipe	150	100
Steel/PVC pipe	38	400
Plexiglass pipe	0.041	/

Mathematical modeling

The flux (B, the amount of sediment particles passing through the pipeline per unit time), erosion amount (W, cumulative amount of sediment particles eroded in the pipeline at a certain moment), and erosion rate (φ) of the sediment particles in the pipeline were calculated using the SS concentration and flow of the water sample and Equations (1)–(3):

$$B_i = \frac{C_i \times Q_i}{3600} \tag{1}$$

$$W_i = \frac{(B_i + B_{i-1})}{2000} \times (t_i - t_{i-1}) + W_{i-1} \tag{2}$$

$$\phi_i = \frac{W_i}{W_0} \times 100 \quad (\%) \tag{3}$$

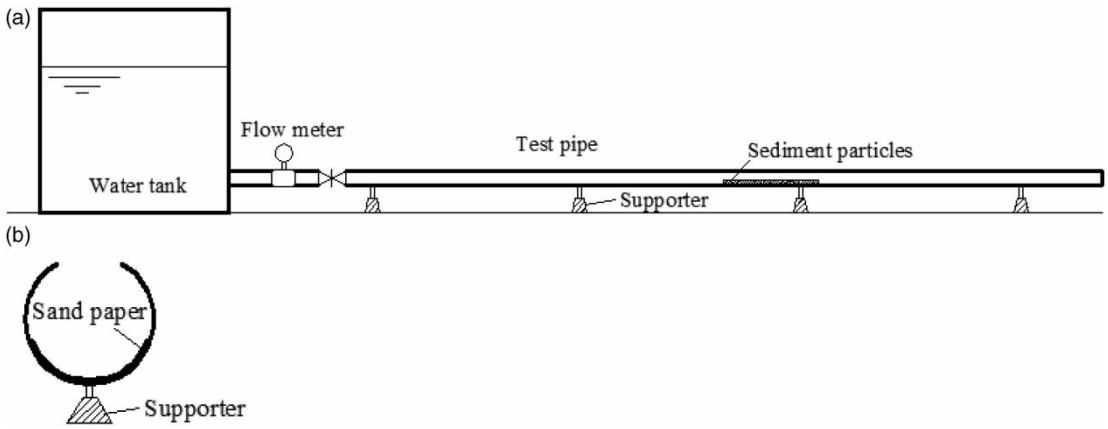

Figure 1 | Simulation test device. (a) Side view of the device; (b) sectional view of the pipe.

where B_i is the amount of sediment particles passing through the pipeline per unit time at the time i (mg/s), C_i is the SS concentration of the sample at the time i (mg/L), Q_i is the flow at the time i (L/h), t_i is the erosion time (s), W_i is the cumulative amount of sediment particles eroded in the pipeline at the time i (g), and W_0 is the initial total mass of sedimentary particles (g).

The principles and methods of fluid mechanics and probability statistics were used in this work based on the experimental and computational data. The mathematical models describing the erosion process were developed using Matlab 9.0 (R2016a). The mathematical models for calculating the critical velocity of different pipes in the erosion process were established through statistical analysis and data fitting.

$$V_L = f(x) \tag{4}$$

where V_L is the migration critical velocity in the erosion process (m/s), and x is the parameter related to pipeline and sediment conditions, such as particle size (d_{50}, median diameter, mm), and sediment thickness (h, cm).

The 'critical velocity' is defined in this study as the water flow velocity corresponding to an erosion rate of approximately 10% (specifically in the range of 9.50%–10.50%) when the erosion time is 1 min.

RESULTS

Factors influencing the migration critical velocity of small-sized sediment particles in a rainwater pipeline

The critical velocity at which the sediment particles are going to start eroding in the rainwater pipeline is affected by many factors: the three factors, namely, particle sizes (d_{50}), pipe wall roughness (μ), and sediment thickness (h), have a great impact (Hong *et al.* 2016; Aksoy *et al.* 2017; Liu *et al.* 2018). The parameter selection of this study is based on the data from the literature (Table 2).

The effect of sediment particle size on the migration critical velocity is shown in Figure 2(a). Under the same conditions, the critical velocity is small when the particle size is large; that is, within the smaller range of 0.33 mm to 0.83 mm. When the particle size decreases from 0.83 mm to 0.33 mm, the critical velocity increases from 0.441 m/s to approximately 0.530 m/s.

Table 2 | Ranges of experimental parameters

Input variable	Input value	Research content and source
Flow	720–1,440 L/h	Solids transport (Walski *et al.* 2009)
Pipe wall roughness	400 μm, 2.55–14.91 μm	Flow and sedimentation dynamics (Lange & Wichern 2013; Cowle *et al.* 2019)
Sediment thickness	0.081–10 cm, 0.3–0.45 cm	Sediments in sewer (Bong *et al.* 2016; Larrarte *et al.* 2016)
Median particle size	0.006–2 mm, 0–0.40 mm	Heavy metals in sediments (Li *et al.* 2010), urban washoff process with physical modeling (Hong *et al.* 2016)

At the same particle size, the large flow velocity has large flow energy. Therefore, the large flow velocity has a high erosion rate. For example, under the particle size of 0.83 mm, the flow velocity increases from 0.387 m/s to 0.481 m/s, and the erosion rate increases from 6.16% to 13.22%. When the particle size is 0.33 mm, the flow velocity increases from 0.497 m/s to 0.553 m/s, and the erosion rate increases from 6.75% to 12.88%.

Rainwater pipes have different pipe wall roughnesses due to diverse pipe materials, rainwater quality, or service life. The four roughnesses in Figure 2(b) correspond to the four commonly used pipes (Table 1). The pipe wall roughness has a great impact on the migration critical velocity. The critical velocity significantly decreases with the decrease of roughness. The pipe wall roughnesses of 250, 150, 38, and 0.041 μm correspond to the critical velocities of 0.864, 0.781, 0.553, and 0.441 m/s, respectively.

The different sediment thickness in the pipeline will also bring about the changes in the migration critical velocity. Figure 2(c) studies the relationship between the two. Evidently, the critical velocity changes in the same direction as the sediment thickness, that is, the critical velocity is small when the sediment thickness is also small. In this study, the change of sediment thickness is small. When the thickness reduces from 0.35 cm to 0.20 cm, the critical velocity decreases from 0.497 m/s to 0.418 m/s.

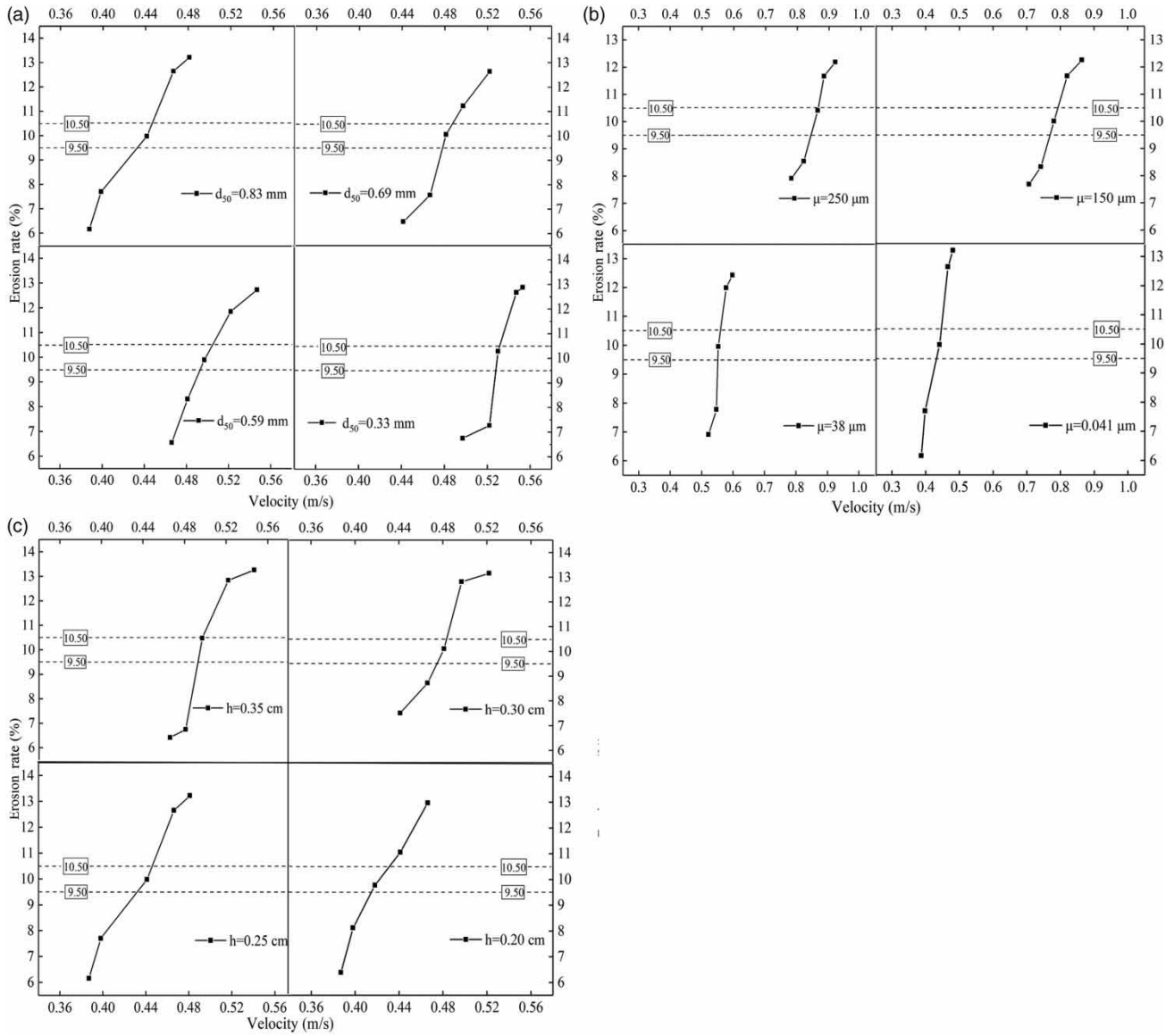

Figure 2 | Influencing factors of the migration critical velocity. (a) Sediment particle size ($\mu = 0.041$ μm, $h = 0.25$ cm); (b) pipe wall roughness ($d_{50} = 0.83$ mm, $h = 0.25$ cm); (c) sediment thickness ($d_{50} = 0.83$ mm, $\mu = 0.041$ μm).

Migration critical velocity of the four types of pipes

When the particle size, pipe wall roughness, and sediment thickness are within a certain range, the range of the critical velocity in pipelines is obtained through experiments. Figure 3 lists the critical velocity ranges of the four types of pipes when the particle size is between 0.33 mm and 0.83 mm, and the sediment thickness is between 0.20 cm and 0.35 cm. In summary, the minimum and maximum values of the critical velocity gradually increase with the roughness increase. When the roughness increases from 0.041 μm (plexiglass pipe) to 250 μm (cast iron pipe), the minimum value increases from 0.418 m/s to 0.820 m/s, and the maximum value increases from 0.561 m/s to 1.195 m/s, both of which almost have been doubled.

Figure 3 shows that the range of the critical velocity also increases with the roughness increase. The variation rate between the maximum and the minimum values in the

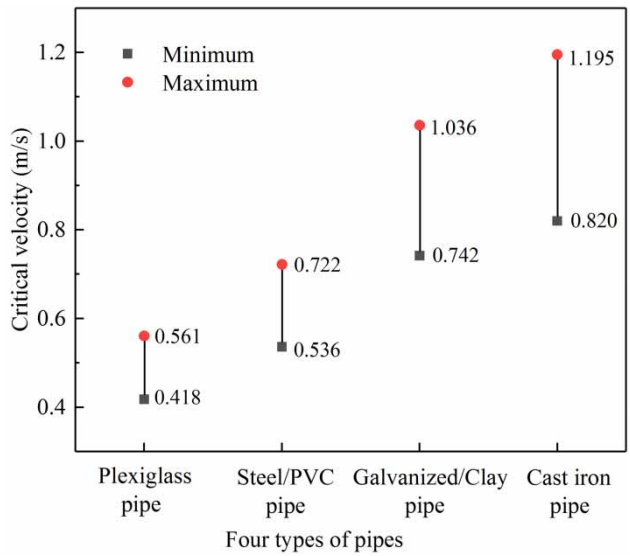

Figure 3 | Migration critical velocity ranges of the four types of pipes.

critical velocity range of each pipe has been calculated. The variation rates of the four pipes, namely, plexiglass pipe, steel/PVC pipe, galvanized/clay pipe, and cast iron pipe, are 34.21%, 34.70%, 39.62%, and 45.73%, respectively. Under large roughness, when the particle size or sediment thickness changes, more complex erosion characteristics are shown, thereby making the critical velocity span large.

Mathematical models for the migration critical velocity of small-sized sediment particles

The calculation models of the migration critical velocity for each pipe under four particle sizes were established by statistical analysis and data fitting (Table 3).

The general formula is shown in Equation (5):

$$V_L = a \cdot h^b \tag{5}$$

where V_L and h are the same as in Equation (4), and a and b are constants reflecting the differences in the pipe material and particle size.

The quadratic fitting of the migration critical velocity was performed in Table 3. Take the plexiglass pipe as an example, there were four values of a (0.7027, 0.7223, 0.7124 and 0.7048) and four values of b (0.3258, 0.3003, 0.2479 and 0.2125) corresponding to the four particle sizes ($d_{50} = 0.83$ mm, 0.69 mm, 0.59 mm and 0.33 mm). The functional relationship between constants a or b and the particle size of the sediment were established, respectively:

Table 3 | Calculation models of the migration critical velocity of sediment in the rainwater pipe

Pipe	d_{50} (mm)	Calculation models for V_L	R^2
Plexiglass pipe	0.83	$0.7027h^{0.3258}$	0.9775
	0.69	$0.7223h^{0.3003}$	0.9764
	0.59	$0.7124h^{0.2479}$	0.9538
	0.33	$0.7048h^{0.2125}$	0.9787
Steel/PVC pipe	0.83	$0.8370h^{0.2881}$	0.9021
	0.69	$0.8802h^{0.2928}$	0.8942
	0.59	$0.9102h^{0.2860}$	0.7785
	0.33	$0.9720h^{0.3166}$	0.7827
Galvanized/clay pipe	0.83	$1.3950h^{0.4013}$	0.9743
	0.69	$1.3890h^{0.3654}$	0.9761
	0.59	$1.3270h^{0.2675}$	0.9801
	0.33	$1.2930h^{0.2205}$	0.9336
Cast iron pipe	0.83	$1.5660h^{0.4167}$	0.9213
	0.69	$1.7580h^{0.4785}$	0.8981
	0.59	$1.8270h^{0.4644}$	0.9683
	0.33	$1.8600h^{0.4342}$	0.9477

$$a = -5.726 \times 10^{-17} e^{40.55 d_{50}} + 0.6894\, e^{0.063 d_{50}} \tag{6}$$

$$b = 0.1385\, e^{1.049 d_{50}} + 89.25\, e^{-39.98 d_{50}} \tag{7}$$

Equations (6) and (7) were substituted into (5), and the mathematical model of the migration critical velocity of plexiglass pipe was established as Equation (8).

$$V_L = (-5.726 \times 10^{-17} e^{40.55 d_{50}} + 0.6894 e^{0.063 d_{50}}) \times h^{(0.1385 e^{1.049 d_{50}} + 89.25 e^{-39.98 d_{50}})} \tag{8}$$

In the same way, the mathematical models of the other three pipes were established as Equations (9)–(11).

Steel/PVC pipe:

$$V_L = (-0.255 e^{-4.894 d_{50}} + 1.163 e^{-0.39 d_{50}}) \times h^{(1.221 \times 10^8 e^{-67.07 d_{50}} + 0.2848\, e^{0.021 d_{50}})} \tag{9}$$

Galvanized/clay pipe:

$$V_L = (-2.557 \times 10^{-17} e^{40.87} d_{50} + 1.212 e^{0.181} d_{50}) \times h^{(0.12 e^{1.484} d_{50} + 1.814 \times 10^4 e^{40.97} d_{50})} \quad (10)$$

Cast iron pipe:

$$V_L = (-0.03672 e^{3.568} d_{50} + 1.805 e^{0.2789} d_{50}) \times h^{(-4.614 \times 10^{-17} e^{42.27} d_{50} + 0.3971 e^{0.269} d_{50})} \quad (11)$$

The migration critical velocity under a certain sediment thickness and particle size could be calculated according to Equations (8)–(11).

Comparison between the calculated and the measured values of the migration critical velocity

Equations (8)–(11) were used to calculate the critical velocity of the erosion under different conditions and to compare with the experimental measured values under the same conditions. The results shown in Figures 4–7 correspond to the above-mentioned four types of pipes.

Figures 4–7 display the calculated and measured values under different conditions, and the difference rates between the two are also shown. Under different particle sizes, roughnesses, and sediment thicknesses, the difference rates between the calculated and the measured values are in the range of −3.60% to 5.33%. Globally, the simulation results

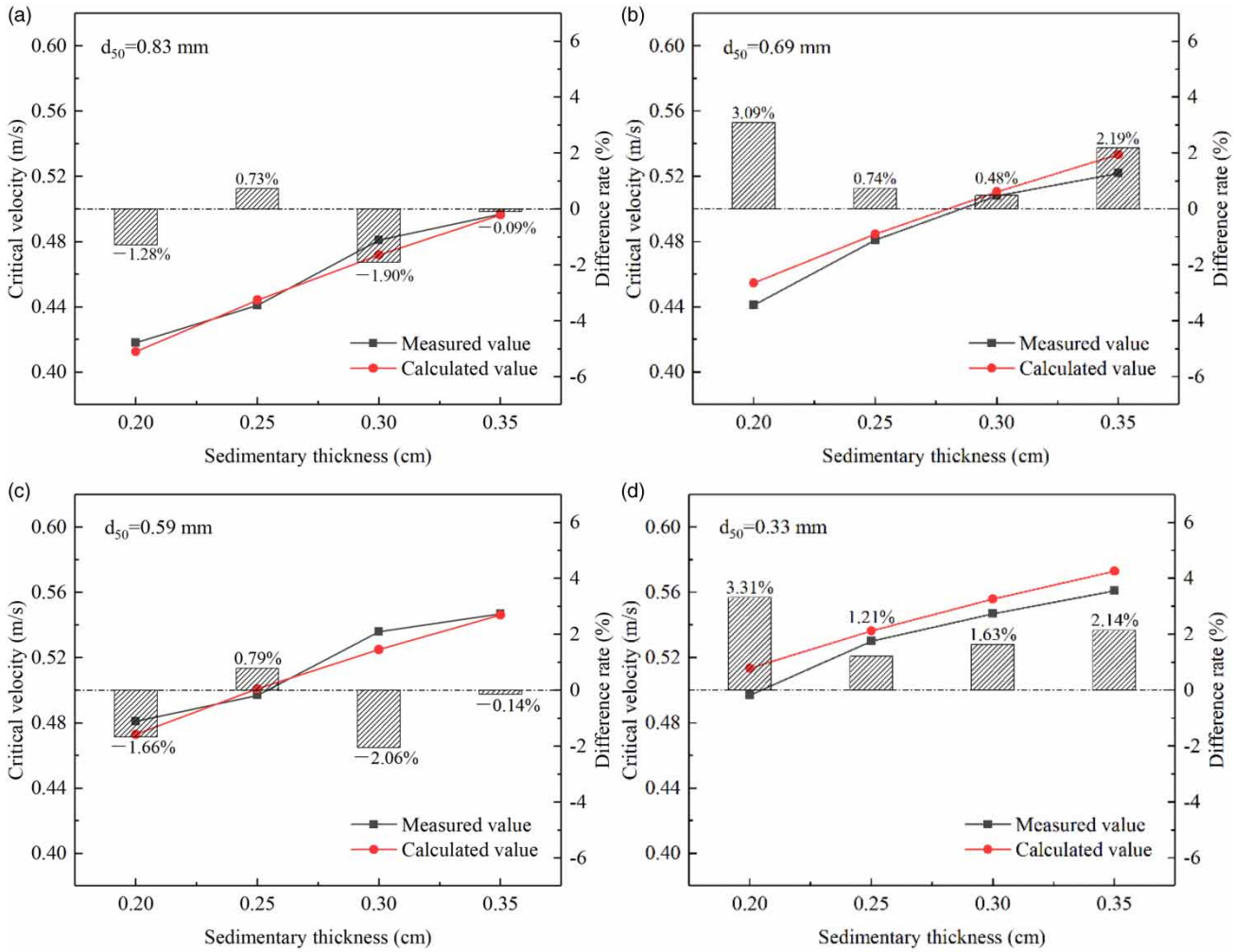

Figure 4 | Comparison between the calculated and the measured values of the critical velocity for plexiglass pipe. (a) $d_{50} = 0.83$ mm; (b) $d_{50} = 0.69$ mm; (c) $d_{50} = 0.59$ mm; (d) $d_{50} = 0.33$ mm.

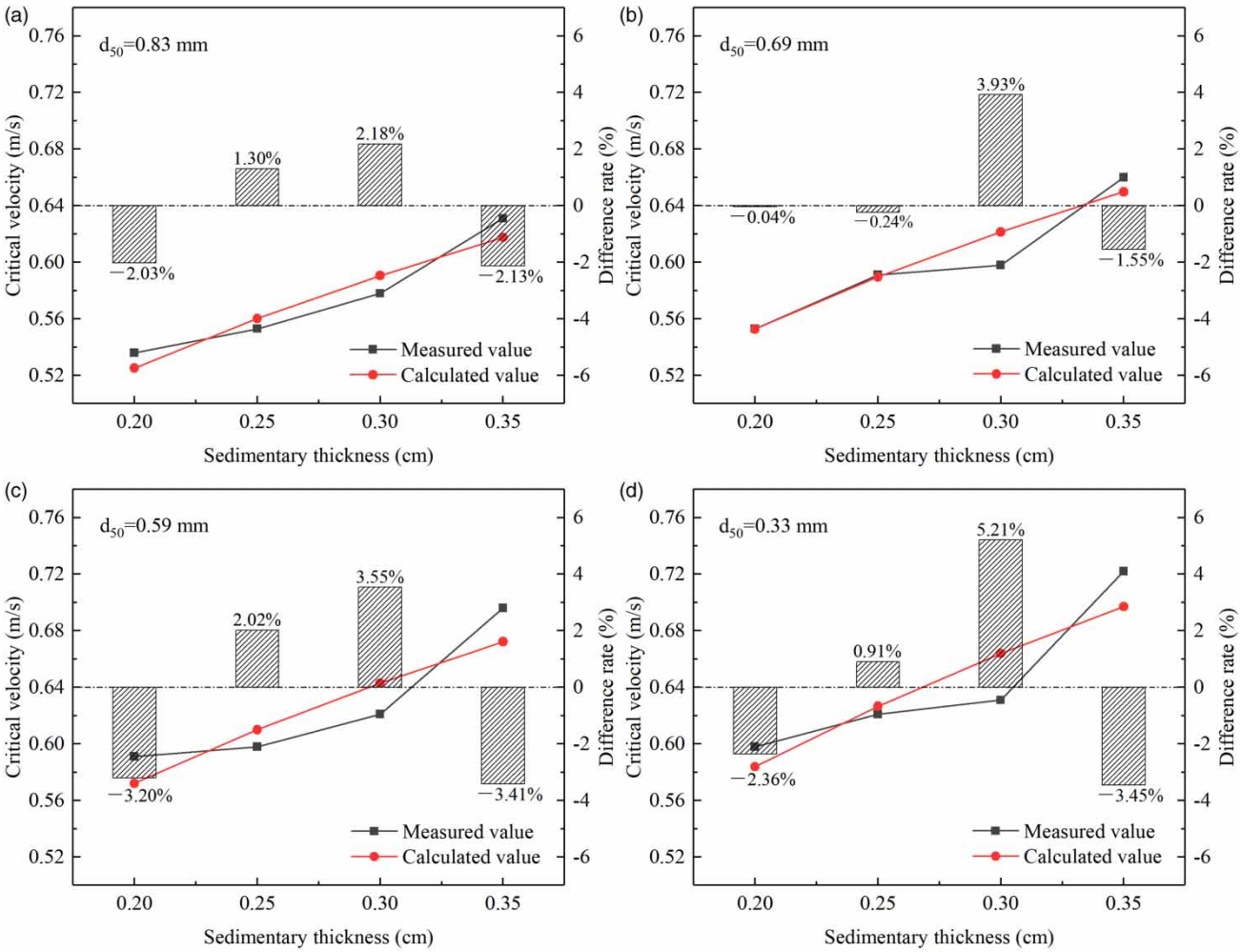

Figure 5 | Comparison between the calculated and the measured values of the critical velocity for steel/PVC pipe. (a) $d_{50} = 0.83$ mm; (b) $d_{50} = 0.69$ mm; (c) $d_{50} = 0.59$ mm; (d) $d_{50} = 0.33$ mm.

show a good agreement with the experimental data. The established mathematical models can efficiently simulate the critical state of erosion in the rainwater pipeline.

DISCUSSION

Factors influencing the migration critical velocity of small-sized sediment particles in a rainwater pipeline

Highly aggregated soils have been proven to be resistant to water erosion (Shi *et al.* 2010; Mahmoodabadi & Ahmadbeigi 2013). When the sediment particles are fine, the adhesive force is strong, and the agglomerates that they form can greatly resist erosion (Eshel *et al.* 2004). The results showed that the high water flow dynamic and rainfall intensity often lead to high water erosion (Defersha & Melesse 2012; Shi *et al.* 2012; Guo *et al.* 2018). It was also proposed that rainfall intensity had a greater impact on the distribution of sediment particles than slope (Berger *et al.* 2010). When other conditions remain unchanged, the high water flow or rainfall intensity could bring great water flow velocity, which can efficiently erode the sediment on the slope or in the pipeline.

When the water flow dynamic is sufficiently large, the aggregates formed by the sedimentary particles can be disintegrated and transported. A threshold for rainfall intensity was found, beyond which the disintegration of aggregates

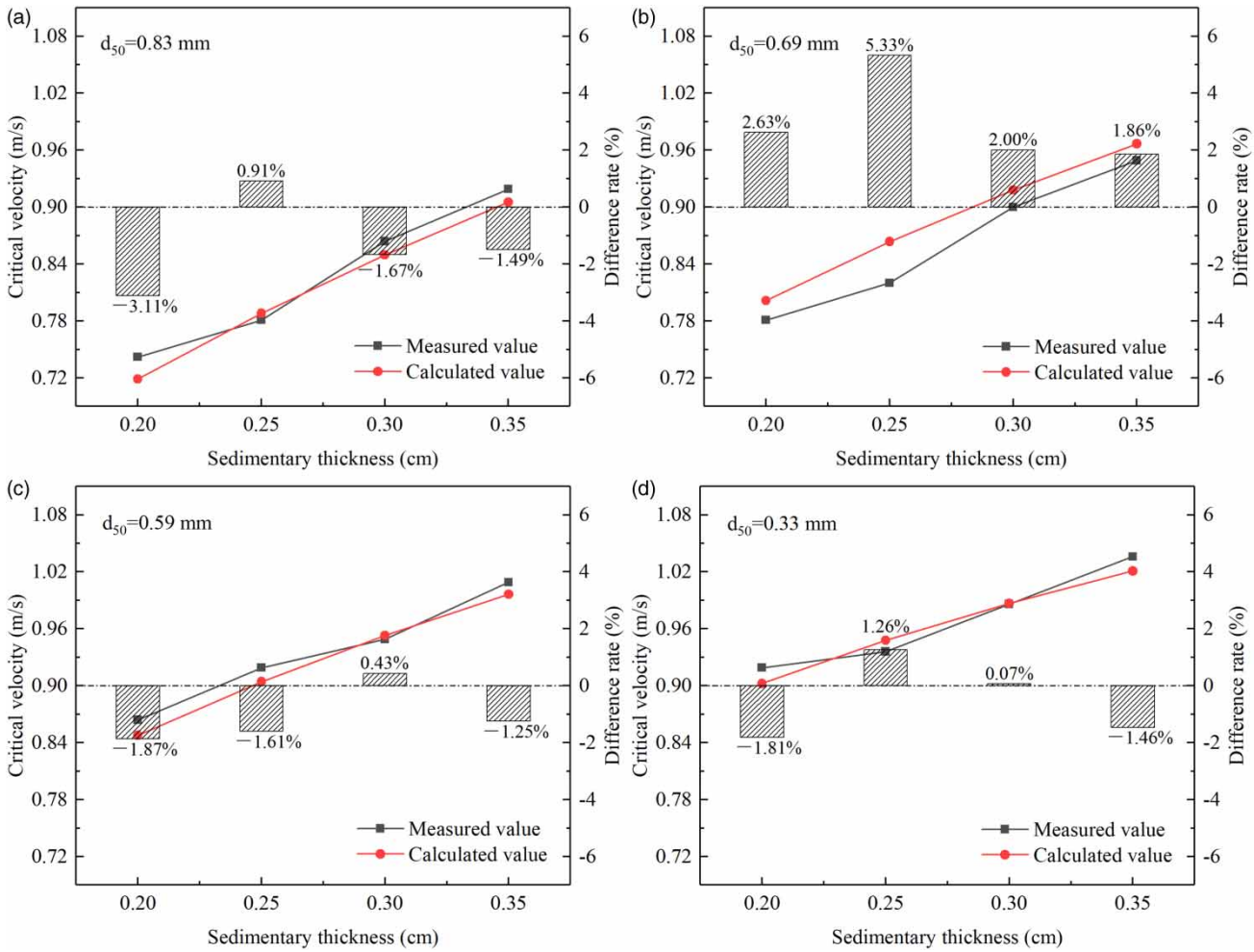

Figure 6 | Comparison between the calculated and the measured values of the critical velocity for galvanized/clay pipe. (a) $d_{50} = 0.83$ mm; (b) $d_{50} = 0.69$ mm; (c) $d_{50} = 0.59$ mm; (d) $d_{50} = 0.33$ mm.

(particle size > 0.25 mm) would be serious (Wang *et al.* 2016). The high rainfall intensity could release fine particles by breaking up large aggregates (Hao *et al.* 2019). In this study, the sediment aggregates are presumed to have been disintegrated or partially disintegrated when the erosion rate has reached 10%. Therefore, the erosion rate of 10% was used as an evaluation index.

The sediment particles in this study belong to the category of small particle size ($d_{50} = 0.33$–0.83 mm), and all have strong viscosity. When the median particle size is small, the content of fine particles is high, the cohesive force is strong, and aggregates are difficult to be eroded and transported. Under the same conditions, small-sized particles need high water flow dynamic to be washed away and floated; thus, the critical velocity is large (Figure 2(a)). The effects of the hydraulic conditions, river bed roughness, and particle composition were considered during the study of the starting conditions of non-uniform sediment particles on the river bed. The coarse particles were easy to start, and the fine particles were difficult to start (He *et al.* 2002).

Once disintegration occurred, the transport mechanism between the fine and the coarse particles differed. During the erosion of red soil by rainfall runoff, sediments with a particle size of <0.1 mm were transferred in the form of suspension/jump, whereas large sediments with a particle size of 0.5–2 mm were transferred in the rolling form (Wu *et al.* 2017). It was pointed out that the particle size of

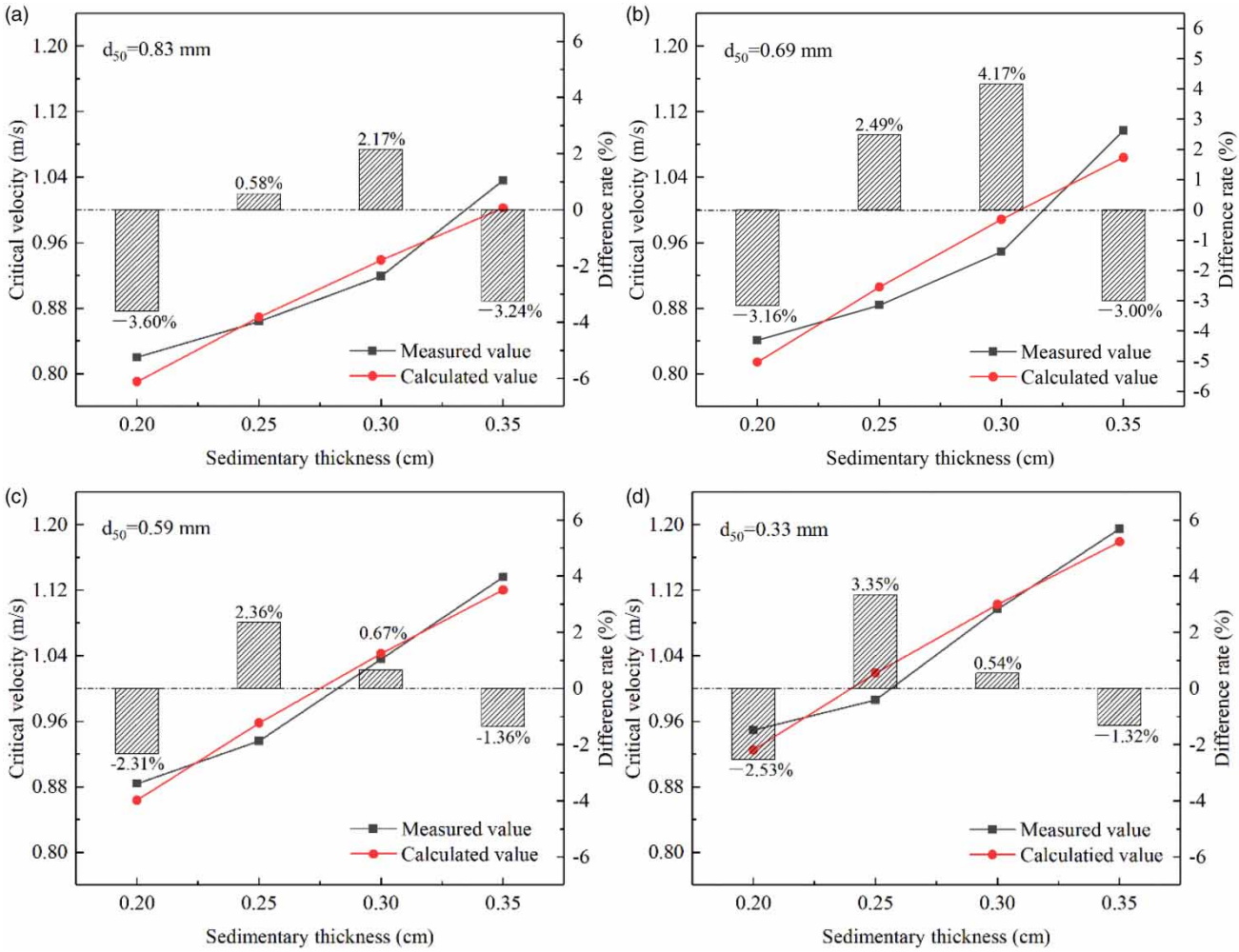

Figure 7 | Comparison between the calculated and the measured values of the critical velocity for cast iron pipe. (a) $d_{50} = 0.83$ mm; (b) $d_{50} = 0.69$ mm; (c) $d_{50} = 0.59$ mm; (d) $d_{50} = 0.33$ mm.

sediment transported in the form of suspension/jump was approximately <0.05 mm under rainfall conditions (Hao *et al.* 2019). In this study, the median particle size was in the range of 0.33 mm to 0.83 mm, and the transport of both forms should exist after the aggregate collapse.

When the bed roughness increased, the energy loss increased due to the exchange of the fluid and the boundary (Cheng *et al.* 2016). The frictional resistance of the sedimentary particles on the pipe wall was great with the increase of the friction coefficient (Cheng *et al.* 2016). The soil surface roughness had a significant delayed effect on runoff generation during the study of the effect of soil surface roughness on runoff; the surface runoff was difficult to form when roughness increased (Ding & Huang 2017). The soil surface roughness also affected the threshold flow of wind and water erosion, which increased with the increase of roughness (Bullard *et al.* 2018).

When the flow or velocity increases to a certain extent, the particles begin to 'start'. Therefore, a larger wall roughness has a great critical velocity, which will also consume a substantial amount of energy (Figure 2(b)). It was found that the particle's movement on the pipe wall was blocked due to the pipe roughness, and a substantial amount of energy was consumed to maintain the state of continued movement (Li *et al.* 2019). The motion of large particles in the drainage pipe was studied, and it was concluded that increasing the flow rate would easily cause the particles to move (Walski *et al.* 2009).

When the erosion rate of a large deposition thickness reaches the same 10%, the absolute amount of particles floating by eroding is great, and the water flow dynamic is needed (Caviedes-Voullieme *et al.* 2017).

Migration critical velocity of the four types of pipes

In general, the minimum and maximum values of the critical velocity gradually increase with the increase of pipe roughness (Figure 3). The above-mentioned analysis indicated that when the roughness of the pipe is large, it will cause a large resistance to the water flow, thereby resulting in the decline of the water flow dynamic (Celmer *et al.* 2008; Cheng *et al.* 2016; Bullard *et al.* 2018). A high flow velocity is required to make the particles 'start'. The erosion characteristics become complicated with the roughness increase, thereby making the range span of the critical velocity large.

Fitting calculation for the migration critical velocity

The critical velocity ranges for the four pipes are calculated on the basis of the studied particle size and sediment thickness by using the mathematical models (Equations (8)–(11)): 0.413–0.573 m/s for the plexiglass pipe, 0.525–0.697 m/s for the steel/PVC pipe, 0.719–1.021 m/s for the galvanized/clay pipe, and 0.790–1.179 m/s for the cast iron pipe (Figures 4–7).

The starting conditions of sediment in the bottom bed of natural rivers were simulated and studied; the results indicated that the starting velocity of sediment with a particle size between 0.75 mm and 3.5 mm was within the range of 0.1–0.5 m/s under different slopes (He *et al.* 2003). When the particle size is in a large range (i.e. 0.001–10 mm), the starting velocity is in the range of 0.02–1.0 m/s (He *et al.* 2002).

The flow velocity in the drainage pipes that can continuously move large particles (referring to the vertical height of the particles being greater than the water depth in the pipe) is in the range of 0.6–1.0 m/s (Walski *et al.* 2009). A sediment erosion test was carried out in a channel with a length of 1.24 km (sediment particle size distribution: $d_{30} = 0.3$ mm, $d_{50} = 1$ mm, and $d_{90} = 10$ mm; and sediment thickness of 1–10 cm). When the flow velocity was approximately 1 m/s, 50–75% of the inner surface area of the middle and lower reaches of the channel would be covered with sedimentary particles from upstream erosion (Caviedes-Voullieme *et al.* 2017).

CONCLUSIONS

In this study, the sediment particles in the rainwater pipeline may migrate due to water erosion. The flow velocity corresponding to the erosion rate of 10% is taken as the migration critical velocity. The critical velocity of sediment particles with small size presents regularity under different particle sizes, pipe wall roughnesses, and sediment thicknesses.

The sediment particles in the rainwater pipeline are viscous. The cohesive force of particles with a small size is relatively strong. The formed aggregates also have strong erosion resistance. The critical velocity is great when the particle size is small ($d_{50} = 0.33$–0.83 mm). The critical velocity significantly decreases with the decrease in the pipe wall roughness. When the deposition thickness is large, the absolute number of particles floating and transporting corresponding to the erosion rate of 10% is great; thus, the migration critical velocity is also large. Under the research conditions, the migration critical velocities of small-sized sediment particles in pipes with four types of wall roughness have been determined: 0.413–0.573 m/s for the plexiglass pipe, 0.525–0.697 m/s for the steel/PVC pipe, 0.719–1.021 m/s for the galvanized/clay pipe, and 0.790–1.179 m/s for the cast iron pipe. The mathematical models for calculating the migration critical velocity of small-sized sediment particles in rainwater pipelines were established through quadratic fitting. Under the conditions of this study, the difference rate between the calculated and the measured values is in the range of −3.60% to 5.33%, thereby showing a good consistency between the two.

ACKNOWLEDGEMENTS

This work was supported by the National Natural Science Foundation of China (51808285).

DATA AVAILABILITY STATEMENT

All relevant data are included in the paper or its Supplementary Information.

REFERENCES

Ab. Ghani, A. & Md. Azamathulla, H. 2011 Gene-expression programming for sediment transport in sewer pipe systems. *J. Pipeline Syst. Eng.* **2** (3), 102–106.

Aksoy, H., Safari, M. J. S., Unal, N. E. & Mohammadi, M. 2017 Velocity-based analysis of sediment incipient deposition in rigid boundary open channels. *Water Sci. Technol.* **76** (9), 2535–2543.

Berger, C., Schulze, M., Rieke-Zapp, D. & Schlunegger, F. 2010 Rill development and soil erosion: a laboratory study of slope and rainfall intensity. *Earth Surf. Processes Landforms* **35** (12), 1456–1467.

Bong, C. H. J., Lau, T. L., Ab. Ghani, A. & Chan, N. W. 2016 Sediment deposit thickness and its effect on critical velocity for incipient motion. *Water Sci. Technol.* **74** (8), 1876–1884.

Bullard, J. E., Ockelford, A., Strong, C. L. & Aubault, H. 2018 Impact of multi-day rainfall events on surface roughness and physical crusting of very fine soils. *Geoderma* **313**, 181–192.

Campisano, A., Creaco, E. & Modica, C. 2004 Experimental and numerical analysis of the scouring effects of flushing waves on sediment deposits. *J. Hydrol.* **299** (3/4), 324–334.

Caviedes-Voullieme, D., Morales-Hernandez, M., Juez, C., Lacasta, A. & Garcia-Navarro, P. 2017 Two-dimensional numerical simulation of bed-load transport of a finite-depth sediment layer: applications to channel flushing. *J. Hydraul. Eng.* **143** (9), 04017034.

Celmer, D., Oleszkiewicz, J. A. & Cicek, N. 2008 Impact of shear force on the biofilm structure and performance of a membrane biofilm reactor for tertiary hydrogen-driven denitrification of municipal wastewater. *Water Res.* **42** (12), 3057–3065.

Cheng, N., Liu, X., Chen, X. & Qiao, C. 2016 Deviation of permeable coarse-grained boundary resistance from Nikuradse's observations. *Water Resour. Res.* **52** (2), 1194–1207.

Cowle, M. W., Webster, G., Babatunde, A. O., Bockelmann-Evans, B. N. & Weightman, A. J. 2019 Impact of flow hydrodynamics and pipe material properties on biofilm development within drinking water systems. *Environ. Technol.* **41** (28), 1–13. https://doi.org/10.1080/09593330.2019.1619844.

Defersha, M. B. & Melesse, A. M. 2012 Effect of rainfall intensity, slope and antecedent moisture content on sediment concentration and sediment enrichment ratio. *Catena* **90**, 47–52.

Ding, W. & Huang, C. 2017 Effects of soil surface roughness on interrill erosion processes and sediment particle size distribution. *Geomorphology* **295**, 801–810.

Ebtehaj, I. & Bonakdari, H. 2013 Evaluation of sediment transport in sewer using artificial neural network. *Eng. Appl. Comput. Fluid* **7** (3), 382–392.

Ebtehaj, I., Bonakdari, H. & Sharifi, A. 2014 Design criteria for sediment transport in sewers based on self-cleansing concept. *J. Zhejiang Univ-Sc. A* **15** (11), 914–924.

Eshel, G., Levy, G. J., Mingelgrin, U. & Singer, M. J. 2004 Critical evaluation of the use of laser diffraction for particle-size distribution analysis. *Soil Sci. Soc. Am. J.* **68** (3), 736–743.

Fletcher, T. D., Andrieu, H. & Hamel, P. 2013 Understanding, management and modelling of urban hydrology and its consequences for receiving waters: a state of the art. *Adv. Water Resour.* **51**, 261–279.

Gunkel, M. & Pawlowsky-Reusing, E. 2017 Field campaign on sediment transport behaviour in a pressure main from pumping station to wastewater treatment plant in Berlin. *Water Sci. Technol.* **75** (9), 2025–2033.

Guo, Z., Ma, M., Cai, C. & Wu, Y. 2018 Combined effects of simulated rainfall and overland flow on sediment and solute transport in hillslope erosion. *J. Soil. Sediment.* **18** (3), 1120–1132.

Hao, H., Wang, J., Guo, Z. & Hua, L. 2019 Water erosion processes and dynamic changes of sediment size distribution under the combined effects of rainfall and overland flow. *Catena* **173**, 494–504.

He, W., Cao, S., Liu, X. & Yang, J. 2003 Incipient condition of uniform sediment on different bed slopes. *Hydro-sci. Eng.* **3**, 23–26.

He, W., Fang, D., Yang, J. & Cao, S. 2002 Study on incipient velocity of sediment. *J. Hydraul. Eng.* **10**, 51–56.

Hong, Y., Bonhomme, C., Le, M. & Chebbo, G. 2016 A new approach of monitoring and physically-based modelling to investigate urban wash-off process on a road catchment near Paris. *Water Res.* **102**, 96–108.

Hrissanthou, V. & Hartmann, S. 1998 Measurements of critical shear stress in sewers. *Wat. Res.* **32** (7), 2035–2040.

Lange, R. L. & Wichern, M. 2013 Sedimentation dynamics in combined sewer systems. *Water Sci. Technol.* **68** (4), 756–762.

Larrarte, F., Szturycz, E., Lebouc, L. & Riochet, B. 2016 New technique for continuous monitoring of sediment height. *Flow Meas. Instrum.* **49**, 40–45.

Li, H., Huang, Y. & Wang, C. 2010 The species distribution of heavy metals in storm sewer sediments in Xicheng district. *Beijing. Environ. Chem.* **29** (3), 416–420.

Li, S., Huai, W., Cheng, N. & Coco, G. 2019 Prediction of mean turbulent flow velocity in a permeable-walled pipe. *J. Hydrol.* **573**, 648–660.

Liu, C., Tan, S., Zhang, X., Yang, Y., Xu, Y. & Xu, Y. 2018 Deposition regularity in a rainwater pipeline based on variable transport flux. *J. Environ. Manage.* **224**, 29–36.

Mahmoodabadi, M. & Ahmadbeigi, B. 2013 Dry and water-stable aggregates in different cultivation systems of arid region soils. *Arab. J. Geosci.* **6** (8), 2997–3002.

Ota, J. J. & Perrusquia, G. S. 2013 Particle velocity and sediment transport at the limit of deposition in sewers. *Water Sci. Technol.* **67** (5), 959–967.

Pallarès, A., Fischer, S., France, X., Pons, M. N. & Schmitt, P. 2016 Acoustic turbidity as online monitoring tool for rivers and sewer networks. *Flow Meas. Instrum.* **48**, 118–123.

Shahsavari, G., Arnaud-Fassetta, G. & Campisano, A. 2017 A field experiment to evaluate the cleaning performance of sewer flushing on non-uniform sediment deposits. *Water Res.* **118**, 59–69.

Shi, Z., Yan, F., Li, L., Li, Z. & Cai, C. 2010 Interrill erosion from disturbed and undisturbed samples in relation to topsoil aggregate stability in red soils from subtropical China. *Catena* **81** (3), 240–248.

Shi, Z. H., Fang, N. F., Wu, F. Z., Wang, L., Yue, B. J. & Wu, G. L. 2012 Soil erosion processes and sediment sorting associated with transport mechanisms on steep slopes. *J. Hydrol.* **454–455**, 123–130.

Walski, T., Edwards, B., Helfer, E. & Whitman, B. E. 2009 Transport of large solids in sewer pipes. *Water Environ. Res.* **81** (7), 709–714.

Wang, W., Yin, S., Xie, Y., Liu, B. & Liu, Y. 2016 Effects of four storm patterns on soil loss from five soils under natural rainfall. *Catena* **141**, 56–65.

Wu, X., Wei, Y., Wang, J., Xia, J., Cai, C., Wu, L., Fu, Z. & Wei, Z. 2017 Effects of erosion degree and rainfall intensity on erosion processes for Ultisols derived from quaternary red clay. *Agr. Ecosyst. Environ.* **249**, 226–236.

Zoppou, C. 2001 Review of urban storm water models. *Environ. Modell. Software* **16** (3), 195–231.

First received 29 May 2020; accepted in revised form 17 November 2020. Available online 30 November 2020